SUPPLEMENTARY MATERIALS

Reagent	Color	Clone	Company	Isotype
Live/Dead Fixable Aqua Stain	AmCyan		Thermo Fisher	
CD3	BV650	UCHT1	BD	IgG1 Mouse, K
CD56	ECD	N901	IOTest (BC)	IgG1 Mouse, K
NKG2C	APC/FITC	REA205	Miltenyi	REA
NKG2A	PeCy7	Z199	IOTest (BC)	IgG2b Mouse, K
KIR2DL1/S1	PeCy5.5	EB6B	IOTest (BC)	IgG1 Mouse, K
KIR2DL2/L3/S2	BV605	CH-L	BD	IgG2b Mouse, K
KIR3DL1	BV711	DX9	BD	IgG1 Mouse, K
KIR3DL1/S1	APCVio770	REA168	Miltenyi	REA
CD107a	BV786	H4A3	BD	IgG1 Mouse, K
IFN-γ	AF700	B27	BD	IgG1 Mouse, K
CD94	APC	NA	Miltenyi	REA
TCRgd	PE	B1	Biolegend	IgG1 Mouse, K
Vd1	APCVio770	REA173	Miltenyi	REA
Vd2	PerCP-Vio 700	REA771	Miltenyi	REA
CD4	Alexa 700	SK3	Biolegend	IgG1 Mouse, K
CD8	BV570	RPA-T8	Biolegend	IgG1 Mouse, K
CD16	BV786/BV421	3G8	Biolegend	IgG1 Mouse, K
FcεRIγ	FITC	NA	Millipore	IgG Rabbit
HLA-E	PE	3D12	Biolegend	IgG1 Mouse, K
HLA-ABC	FITC	REA230	Miltenyi	REA
HLA-BC	FITC	REA672	Miltenyi	REA
HLA-C	PE	DT-9	BD	IgG2b Mouse, K

Supplemental Table 1. Antibodies used for phenotyping and functional analysis.

Supplemental figure 1

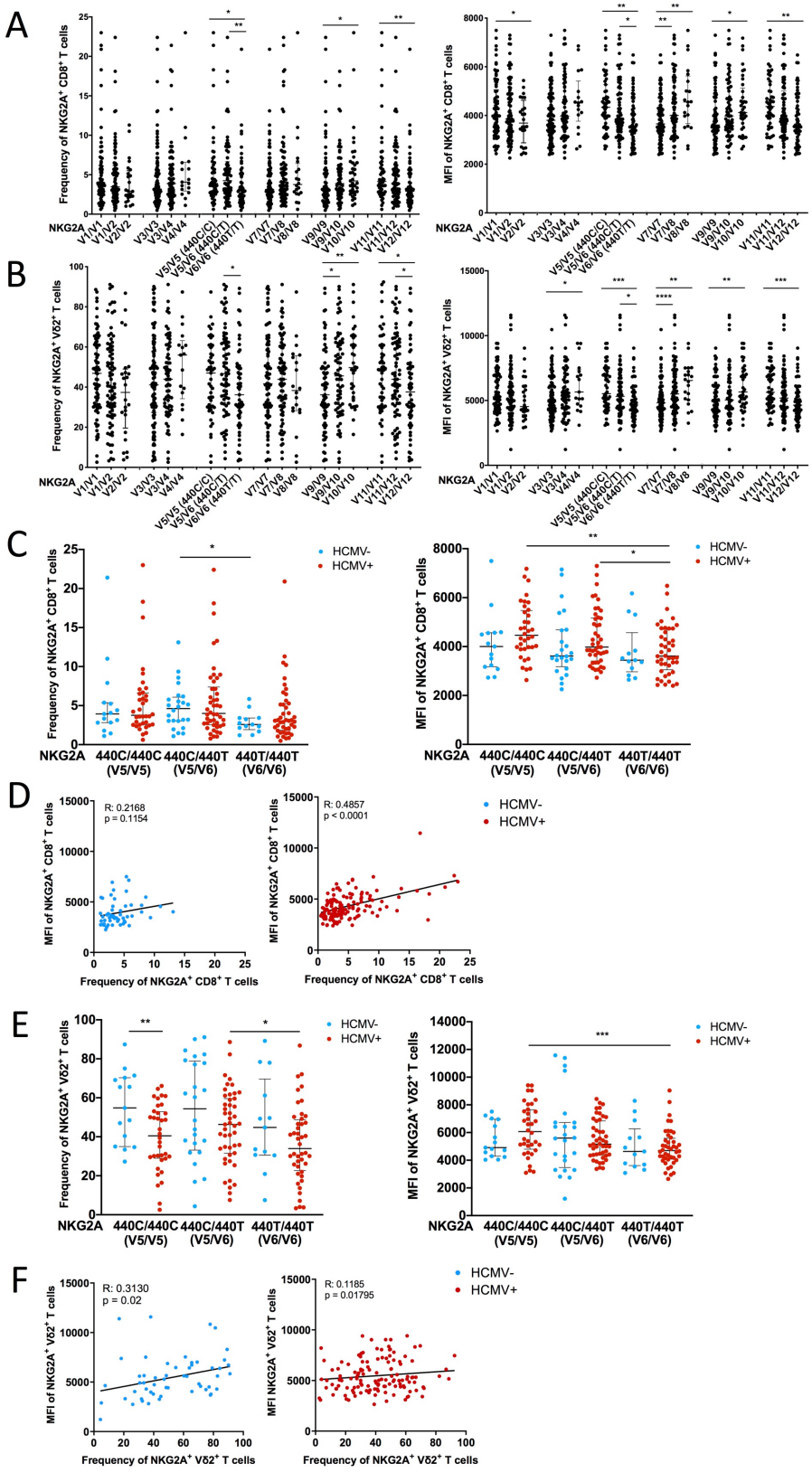

Supplemental Fig. 1. *NKG2A* non-coding SNPs discriminate NKG2A expression on $CD8^+$ T cells and $V\delta2^+$ T cells. (A) NKG2A frequency and MFI of $CD8^+$ T cells grouped by selected *NKG2A* SNPs. (B) NKG2A frequency and MFI of $V\delta2^+$ T cells grouped by selected NKG2A SNPs. (C) NKG2A frequency and MFI of $CD8^+$ T cells stratified by NKG2A 440C/T genotype and HCMV serostatus. (D) Correlation between NKG2A MFI and $NKG2A^+$ frequency among $CD8^+$ T cells in HCMV- (blue), $HCMV^+$ (red) (E) NKG2A frequency and MFI of $V\delta2^+$ T cells stratified by NKG2A 440C/T genotype and HCMV serostatus. (F) Correlation between NKG2A MFI and $NKG2A^+$ frequency among $V\delta2^+$ T cells in $HCMV^-$ (blue), $HCMV^+$ (red). Mann-Whitney tests were performed and median ± IQRs presented panel A-C and E. Correlations were assessed using the Pearson correlation coefficient panel D and F. Symbols represent individual samples. *$p < 0.05$, **$p < 0.01$, ***$p < 0.001$, and ****$p < 0.0001$.

Supplemental figure 2

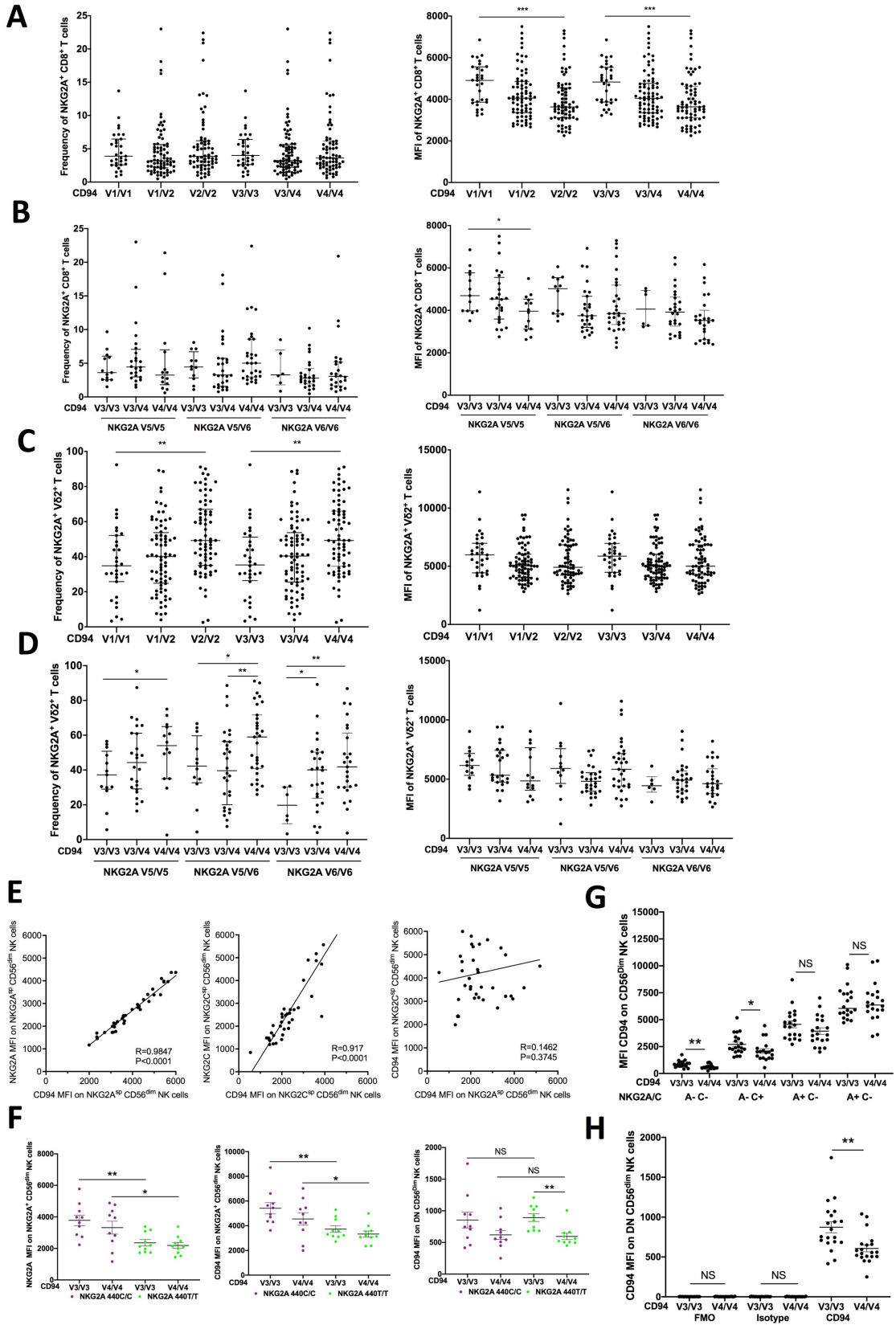

Supplemental Fig. 2. *CD94* polymorphism alone or combined with *NKG2A* polymorphism predicts NKG2A expression on CD8$^+$ T cells and Vδ2$^+$ T cells. (A) CD8$^+$ T cell NKG2A frequency and MFI grouped by *CD94* polymorphism. (B) CD8$^+$ T cell NKG2A frequency and MFI grouped by *CD94* and *NKG2A* polymorphism. (C) Vδ2$^+$ T cell NKG2A frequency and MFI grouped by *CD94* polymorphism. (D) Vδ2$^+$ T cell NKG2A frequency and MFI grouped by *CD94* and *NKG2A* polymorphism. (E) Correlation between NKG2A, NKG2C and CD94 MFI on CD56dim NK cells. (F) NKG2A and CD94 MFI on subpopulations of CD56^{dim} NK cells, stratified by *CD94* SNPs in conjunction with *NKG2A* variants. (G) CD94 MFI stratified by *CD94* SNPs in different CD56^{dim} NK cells population defined by NKG2C and NKG2A positivity. (H) CD94 MFI on DN (NKG2A$^-$NKG2C$^-$) NK cells cell stratified by *CD94* SNPs. Mann-Whitney tests were performed and median ± IQRs presented panel A-D. Correlations were assessed using the Pearson correlation coefficient panel E. T-tests were performed and mean ± SEM presented in panel G-H. Symbols represent individual samples. *$p < 0.05$, **$p < 0.01$, ***$p < 0.001$, and ****$p < 0.0001$.

Supplemental figure 3

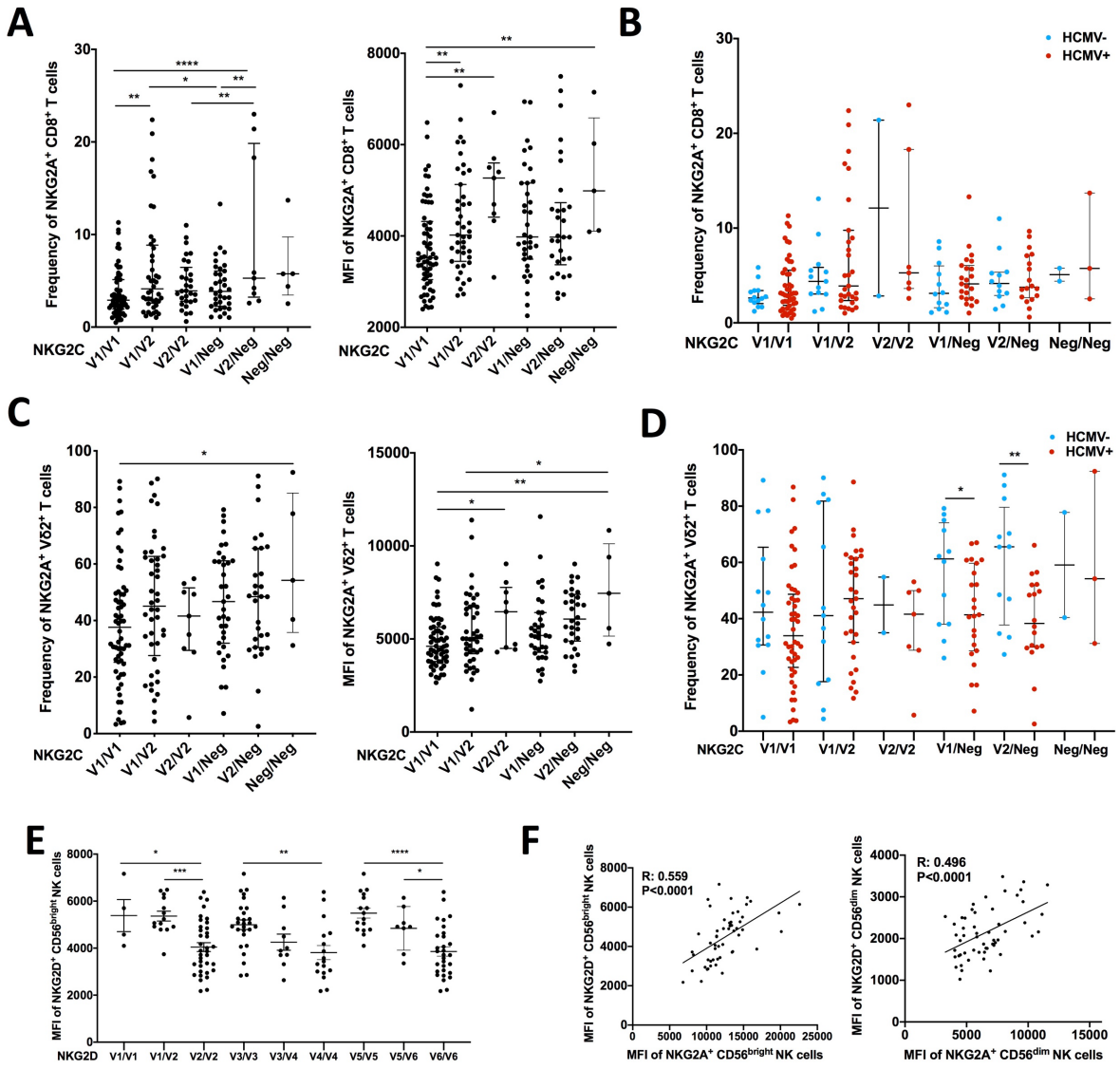

Supplemental Fig. 3. *NKG2C* polymorphism predicts variable NKG2A expression on CD8$^+$ T cells and Vδ2$^+$ T cells. (A) CD8$^+$ T cell NKG2A frequency and MFI grouped by *NKG2C* polymorphism. (B) CD8$^+$ T cell NKG2A frequency and MFI grouped by *NKG2C* polymorphism and HCMV serostatus. (C) Vδ2$^+$ T cell NKG2A frequency and MFI grouped by *NKG2C* polymorphism. (D) Vδ2$^+$ T cell NKG2A frequency and MFI grouped by *NKG2C* polymorphism and HCMV serostatus. (E) NKG2D MFI on CD56^{bright} NK cells stratified by *NKG2D* SNPs. (F)

NKG2D MFI in different NK cell compartments ($CD56^{dim}$ $NKG2A^{-}$, $CD56^{dim}$ $NKG2A^{+}$, $CD56^{bright}$) and correlation between NKG2A and NKG2D MFI. Mann-Whitney tests were performed and median ± IQRs presented in panels A-D. T-tests were performed and mean ± SEM presented in panel E. Correlations were assessed using the Pearson correlation coefficient in panel F. Symbols represent individual samples. *$p < 0.05$, **$p < 0.01$, ***$p < 0.001$, and ****$p < 0.0001$.

Supplemental figure 4

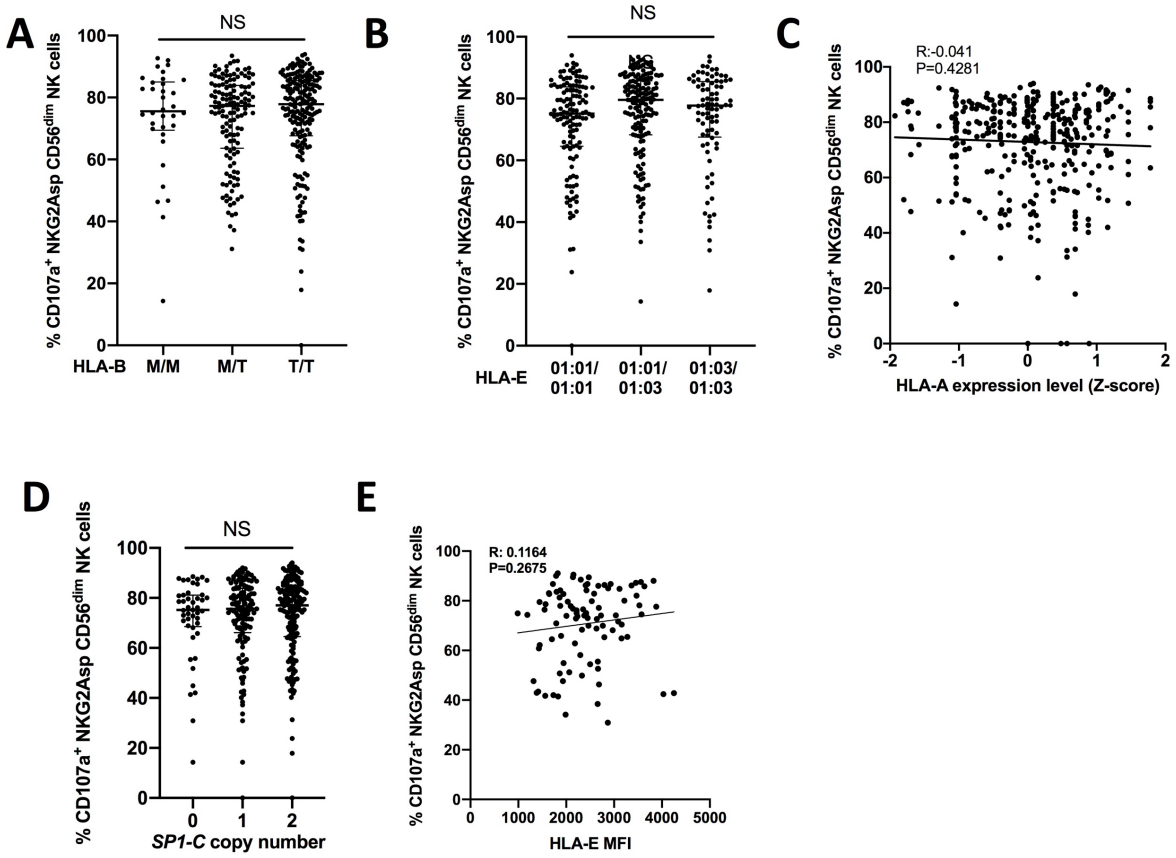

Supplemental Fig. 4. HLA-E expression or scoring methods do not predict NKG2A education on CD56^{dim} NK cells. PBMC from 400 different donors were cultured with K562 HLA-E KO target cells in a CD107a assay. (A) NKG2Asp degranulation frequency stratified by HLA-B leader peptide. (B) NKG2Asp degranulation frequency stratified by HLA-E alleles. (C) NKG2Asp degranulation frequency stratified by HLA-A Z-score. (D) NKG2ASP degranulation frequency stratified by Signal peptide SP-1C. (E) Correlation between HLA-E MFI and NKG2Asp degranulation frequency on PBMC of 100 donors cultured with 721.221 HLA-E KO target cells in a CD107a assay. Mann-Whitney tests were performed and median ± IQRs presented in panels A, B and D. Correlations were assessed using the Pearson correlation coefficient in panels C and E. Symbols represent individual samples. *$p < 0.05$, **$p < 0.01$, ***$p < 0.001$, and ****$p < 0.0001$.

Supplemental figure 5

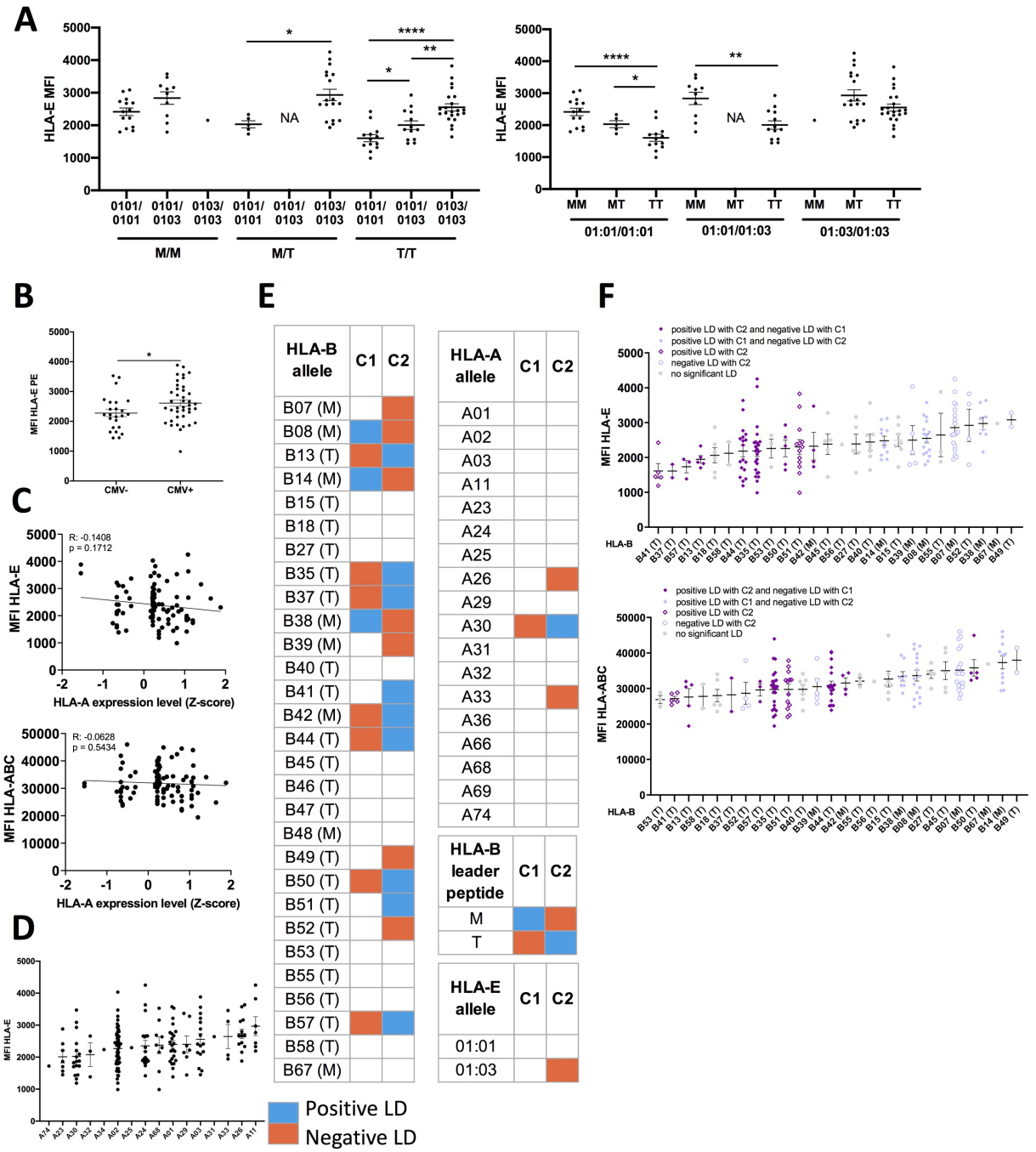

Supplemental Fig. 5. HLA-C epitope is predictive of HLA-E expression and significantly associated with certain HLA-A and HLA-B alleles. (A) HLA-E MFI segregated by HLA-B leader peptide and HLA-E epitope. (B) HLA-E MFI grouped by HCMV serostatus. (C) Correlation

between HLA-A expression level (by calculated Z-score) and HLA-E MFI or HLA-ABC MFI. (D) HLA-E MFI grouped by HLA-A alleles and ranked in croissant order. (E) Linkage disequilibrium between HLA-C epitope, HLA-B alleles, and HLA-A alleles. Positive and negative LD determined at a significance level of <0.05. (F) HLA-E and HLA-ABC MFI grouped by HLA-B alleles, coded by HLA-C epitope found to be in linkage disequilibrium with each allele and ranked in croissant order. HLA-B leader peptide noted in parentheses. T-tests were performed and mean ± SEM presented in panels A and B. Correlations were assessed using the Pearson correlation coefficient in panel C. Linkage Disequilibrium were assessed using Chi-square test (E). Symbols represent individual samples. *$p < 0.05$, **$p < 0.01$, ***$p < 0.001$, and ****$p < 0.0001$.

Supplemental figure 6

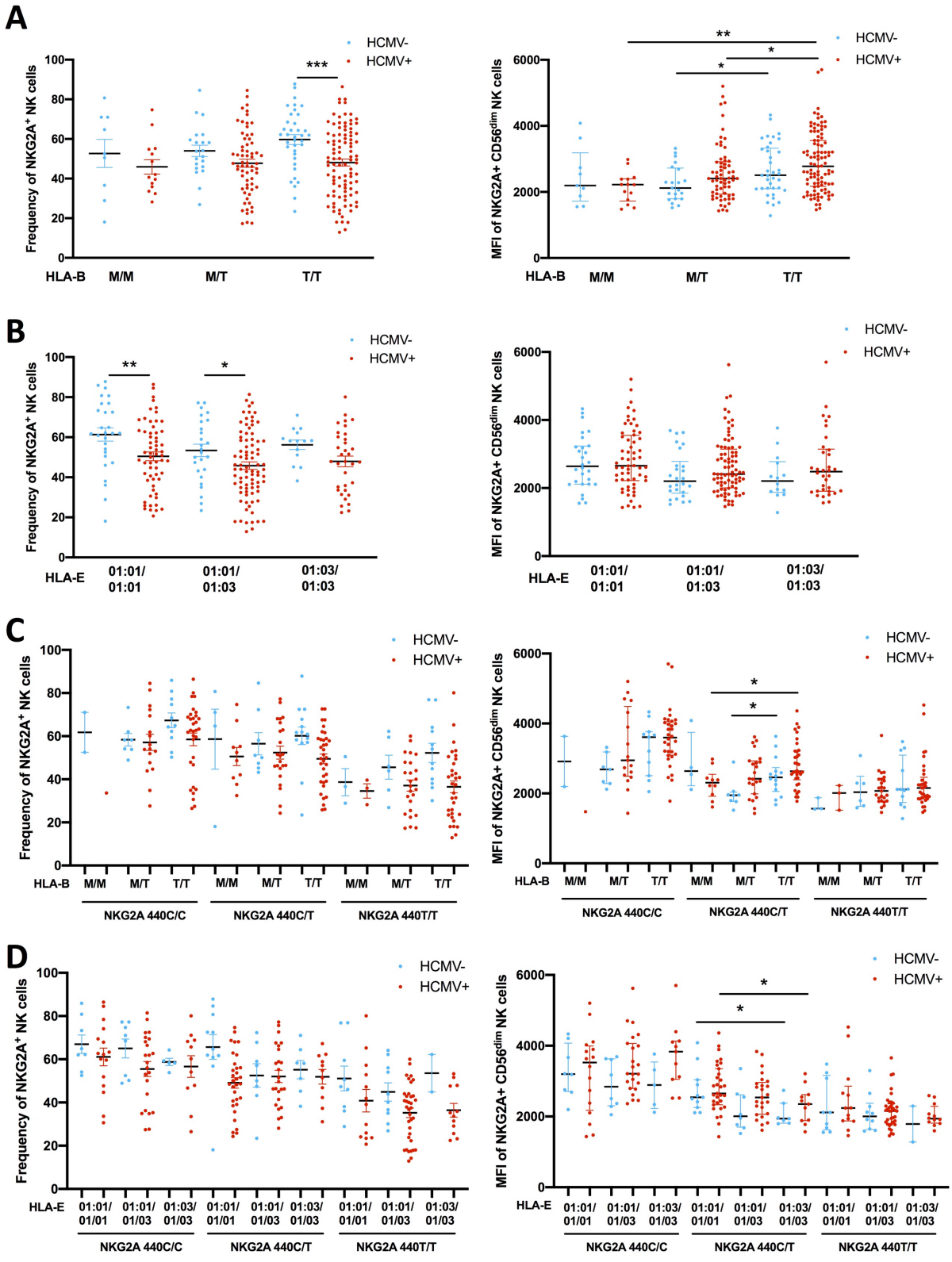

Supplemental Fig. 6. Impact HLA-B leader peptide and HLA-E alleles on NKG2A expression. (A) NKG2A$^+$ NK cell frequency and NKG2A MFI stratified by HLA-B leader peptide and HCMV serostatus. (B) NKG2A$^+$ NK cell frequency and NKG2A MFI stratified by HLA-E alleles and HCMV serostatus. (C) NKG2A$^+$ NK frequency and MFI stratified by HLA-B leader peptide, *NKG2A* SNP genotype, and HCMV serostatus. (D) NKG2A$^+$ NK frequency and MFI stratified by HLA-E alleles, *NKG2A* SNP genotype, and HCMV serostatus. T-tests were performed and mean ± SEM are presented to analyze NKG2A frequencies (A-D). Mann-Whitney tests were performed and median ± IQRs are presented to analyze NKG2A MFI (A-D). Symbols represent individual samples. *$p < 0.05$, **$p < 0.01$, ***$p < 0.001$, and ****$p < 0.0001$.